9-13-2011

Stochastic Modeling of Salt Accumulation in the Root Zone Due to Capillary Flux from Brackish Groundwater

S. H.H. Shah
Wageningen University & Research

R. W. Vervoort
The University of Sydney

S. Suweis
Ecole Polytechnique Fédérale de Lausanne

Andrew J. Guswa
Smith College, aguswa@smith.edu

A. Rinaldo
Ecole Polytechnique Fédérale de Lausanne

See next page for additional authors

Stochastic modeling of salt accumulation in the root zone due to capillary flux from brackish groundwater

S. H. H. Shah,[1] R. W. Vervoort,[2] S. Suweis,[3] A. J. Guswa,[4] A. Rinaldo,[3,5] and S. E. A. T. M. van der Zee[1]

Received 23 July 2010; revised 9 July 2011; accepted 25 July 2011; published 7 September 2011.

[1] Groundwater can be a source of both water and salts in semiarid areas, and therefore, capillary pressure–induced upward water flow may cause root zone salinization. To identify which conditions result in hazardous salt concentrations in the root zone, we combined the mass balance equations for salt and water, further assuming a Poisson-distributed daily rainfall and brackish groundwater quality. For the water fluxes (leaching, capillary upflow, and evapotranspiration), we account for osmotic effects of the dissolved salt mass using Van't Hoff's law. Root zone salinity depends on salt transport via capillary flux and on evapotranspiration, which concentrates salt in the root zone. Both a wet climate and shallow groundwater lead to wetter root zone conditions, which in combination with periodic rainfall enhances salt removal by leaching. For wet climates, root zone salinity (concentrations) increases as groundwater is more shallow (larger groundwater influence). For dry climates, salinity increases as groundwater is deeper because of a drier root zone and less leaching. For intermediate climates, opposing effects can push the salt balance either way. Root zone salinity increases almost linearly with groundwater salinity. With a simple analytical approximation, maximum concentrations can be related to the mean capillary flow rate, leaching rate, water saturation, and groundwater salinity for different soils, climates, and groundwater depths.

Citation: Shah, S. H. H., R. W. Vervoort, S. Suweis, A. J. Guswa, A. Rinaldo, and S. E. A. T. M. van der Zee (2011), Stochastic modeling of salt accumulation in the root zone due to capillary flux from brackish groundwater, *Water Resour. Res., 47*, W09506, doi:10.1029/2010WR009790.

1. Introduction

[2] Recently, a system analysis framework [*Rodriguez-Iturbe and Porporato*, 2004] has been developed for the stochastic modeling of the soil water balance, in particular for rain-fed semiarid ecosystems. This framework initially did not consider feedback of the groundwater with the root zone soil water dynamics. However, it is apparent that groundwater can be an important and even dominant factor with regard to vegetation development and patterning [e.g., *Lamontagne et al.*, 2005; *Mensforth et al.*, 1994; *Scott et al.*, 2006; *Thorburn and Walker*, 1994; *Walker et al.*, 1993].

[3] During the past 2 years, interactions between groundwater and the root zone have been taken into consideration by *Vervoort and van der Zee* [2008, 2009], *Ridolfi et al.* [2008], *Laio et al.* [2009], and *Tamea et al.* [2009]. *Vervoort and van der Zee* [2008, 2009] considered the water balance for a vegetated soil, but without accounting for the impact of drainage on groundwater levels. This influence of drainage on groundwater levels was taken into consideration by *Ridolfi et al.* [2008], *Laio et al.* [2009], and *Tamea et al.* [2009] for unvegetated and vegetated soil.

[4] Whereas determining the influence of capillary upflow from the groundwater towards the root zone is of interest, in particular for semiarid regions, the related hazards of salt accumulation in the root zone cannot be ignored. Water moving upward from the groundwater toward the root zone due to capillary forces is known to imply a salinization hazard [*Bresler et al.*, 1982; *Howell*, 1988], and therefore, shallow groundwater and water logging situations need to be avoided [*Berret-Lennard*, 2003; *Datta and Jong*, 2002; *Pichu*, 2006]. This understanding as such is not new. For instance, in Hungary, the depth of the groundwater level is a major factor in assessing the risk of root zone salinity and sodicity [*Szabolcs*, 1989; *Toth*, 2008; *Toth and Szendrei*, 2006; *Van Beek et al.*, 2010; *Varrallyay*, 1989]. The awareness that salts need to be leached to avoid soil salinity is expressed in the concept of leaching fraction as given in the famous work by *Richards et al.* [1954]. This concept has continued to be investigated throughout recent past decades [*Corwin et al.*,

[1]Soil Physics, Ecohydrology and Groundwater Management, Environmental Sciences Group, Wageningen University, Wageningen, Netherlands.
[2]Hydrology Research Laboratory, Faculty of Agriculture, Food and Natural Resources, University of Sydney, Sydney, New South Wales, Australia.
[3]Laboratory of Ecohydrology, IEE, ENAC, École Polytechnique Fédérale, Lausanne, Switzerland.
[4]Picker Engineering Program, Smith College, Northampton, Massachusetts, USA.
[5]Dipartimento IMAGE, Università di Padova, Padua, Italy.

0043-1397/11/2010WR009790

2007; *Rhoades*, 1974; *Rhoades et al.*, 1973]. Besides the leaching fraction, both analytical and numerical modeling approaches for soil salinization have been elaborated, which are complementary in that they emphasize different aspects of the transport phenomena. For instance, *Raats* [1975] considered depth-time trajectories of water particles analytically, considering root water uptake (RWU) and the effect of RWU on salt concentrations. In this analysis, he calculated the depth-time trajectories of elements of water, steady and transient salinity profiles, and responses of salinity sensors at various depths following a step increase and a step decrease of the leaching fraction. An analysis with similarities to that by Raats for linearly adsorbing solutes was presented by *Schoups and Hopmans* [2002] for different scenarios.

[5] In addition to such analytical, or analytically inspired, numerical modeling, fully numerical models have been developed such as UNSATCHEM [*Simunek et al.*, 1996], SWAP [*Kroes et al.*, 2008], and HYDRUS [*Simunek et al.*, 1998, 1999; *Somma et al.*, 1998]. With these tools, it is possible to assess in detail how water flow, solute (salt) transport, and root water uptake affect each other. Although they are computationally more demanding than analytical models, computational power rapidly increases, and this makes this constraint less important.

[6] The scope of this paper is to assess, for a root zone in hydrological contact with groundwater, how salt accumulation is related to root zone water dynamics, with the emphasis on the variability of these dynamics caused by atmospheric forcing. We are interested in the impact of climate drivers such as rainfall intensity, precipitation frequency, and evaporative demand, along with the influence of capillary upflow from the water table. In this work, we presume that the primary source of salt is from groundwater rather than irrigation water, as in the case of *Suweis et al.* [2010].

[7] To keep the emphasis on precipitation timing and intensity, we follow the framework presented by *Rodriguez-Iturbe and Porporato* [2004] and consider the root zone as a single layer without resolving the dynamics of infiltration. *Guswa et al.* [2002, 2004] examined conditions where such a simplification is appropriate; they found that when vegetation has the ability to compensate for heterogeneous distributions of soil moisture, either through hydraulic redistribution or through compensatory uptake, the single-layer and spatially explicit models gave similar results. Such compensation ability has been demonstrated for plants in many different ecosystems [*Caldwell et al.*, 1998; *Dawson*, 1993; *Domec et al.*, 2010; *Green et al.*, 1997; *Katul and Siqueira*, 2010; *Nadezhdina et al.*, 2010; *Oliveira et al.*, 2005].

[8] To understand the development of the salinity of the root zone, we consider a conceptual model of a homogeneous root zone with thickness Z_r (cm), porosity ϕ, and groundwater Z (cm) below the soil surface (Figure 1). The root zone water balance is studied in the probabilistic framework of *Vervoort and van der Zee* [2008] in view of the random character of rainfall. The random fluctuations of root zone water saturation affect the fluctuations of salinity through the contribution of the various fluxes into and out of the root zone, and this balance is the primary scope of this paper.

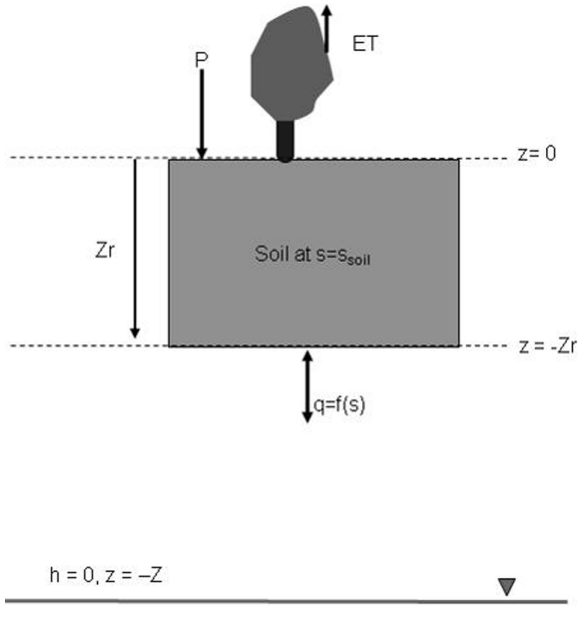

Figure 1. Conceptual model for groundwater uptake by vegetation in a semiarid system.

2. Methods

2.1. Background Theory

[9] Our point of departure is the ecohydrological model including capillary upflow described by *Vervoort and van der Zee* [2008]. Evaporation and rainfall occur at the soil surface and affect mainly the water storage in the root zone. No hysteresis occurs, and the soil water profile below the root zone has a steady state. We assume that the groundwater level is constant, which means that the fluctuations in the groundwater level occur at a much larger time scale than the fluctuations in climate drivers (i.e., years versus days and weeks). We further assume that the soil is initially free from salts and that all salt originates from the groundwater in what commonly is called primary salinization [*Szabolcs*, 1989; *Varrallyay*, 1989].

[10] We have water flow due to rainfall or irrigation P, leaching L, capillary upflow U, and evapotranspiration (ET). This leads to the water balance equation

$$\phi Z_r \frac{\mathrm{d}s}{\mathrm{d}t} = P - \mathrm{ET}(s) + U(s) - L(s), \tag{1}$$

where s is the soil saturation ($0 < s < 1$), and we distinguished all inflow and outflow water fluxes, instead of just a loss function, as they may carry different salt loads.

[11] Rainfall is modeled as a marked Poisson process with a mean storm arrival rate λ (events d^{-1}), and each storm carries a random amount of rainfall [*Rodriguez-Iturbe et al.*, 1999]. Following *Laio et al.* [2001], the climate is subsequently defined by the parameters λ' and γ, which arise from the Poisson distributed daily rainfall. The parameter λ' is equal to $\lambda e^{-\Delta/\alpha}$, where Δ is the interception depth (cm) and α is the mean storm depth (cm event^{-1}). The parameter γ is equal to $\phi Z_r/\alpha$, or equivalently, $1/\gamma$ is the root zone weighted mean storm depth.

[12] The effective normalized water loss function of the root zone (i.e., $\rho = [\mathrm{ET}(s) + L(s) - U(s)]/(\phi Z_r)$), which

also takes into account the effect of the interaction with the groundwater, is [*Vervoort and van der Zee*, 2008]

$$\rho = \begin{cases} (\eta - m_2)\left(\dfrac{s - s_{cr}}{s^* - s_{cr}}\right) & s_{cr} < s \le s^* \\ \eta - m_1\left[1 - e^{\beta(s - s_{\lim})}\right] & s^* < s \le s_{\lim} \\ \eta + m\left[e^{\beta(s - s_{\lim})} - 1\right] & s_{\lim} < s \le 1 \end{cases},$$

$$m_2 = \frac{K_s G}{\phi Z_r}, \qquad (2)$$

$$m_1 = \frac{m_2}{\left[1 - e^{\beta(s^* - s_{\lim})}\right]},$$

$$m = \frac{K_s}{\phi Z_r\left[e^{\beta(1 - s_{\lim})} - 1\right]},$$

$$\eta = \frac{E_{\max}}{\phi Z_r},$$

where the dimensionless parameter G is a function that describes the relationship of the capillary flux with the groundwater depth, the bubbling pressure h_b, and the hydraulic shape parameters α_e and b and has the following functional form [*Eagleson*, 2002]:

$$G = \alpha_e\left(\frac{h_b}{Z - Z_r}\right)^{2+3/b}. \qquad (3)$$

[13] The parameters m_2 and m_1 are constants, where m_2 represents the maximum capillary flux for a given groundwater depth and hydraulic properties (encapsulated in G), while m_1 is equal to m_2 normalized for the reduction in capillary flux with increased saturation. We use β as a soil hydraulic shape parameter, which is related to b, the slope of the water retention curve.

[14] The first important boundary is $s_{\lim}$, which defines the point where, coming from the saturation end, the soil storage moves from leaching L to capillary upflow U, i.e., the point where $L = U = 0$. In other words, at any point wetter than $s_{\lim}$, $U = 0$, and at any point drier than $s_{\lim}$, $L = 0$. If we move from $s_{\lim}$ towards drier conditions, we will reach an important boundary s_{cr}, which depends on the water table depth. This point is the soil saturation for which $U = \mathrm{ET}$ and thus the resultant loss from soil storage is 0. The soil will never dry out below this level of soil saturation because at this point (and below) the potential capillary flux is either equal to or greater than the actual evaporation losses and thus all evaporation demand can be supplied by the capillary flux. Further, s^* is the soil saturation level at which the transpiration becomes limited by available soil moisture, and s_w is soil saturation at wilting point, which is used for calculating s_{cr}. Finally, $E_{\max}$ is the maximum evapotranspiration [*Rodriguez-Iturbe and Porporato*, 2004], and η is the root zone depth normalized version of $E_{\max}$.

[15] Because the loss function (2) is fundamental for this work, we show it in Figure 2 for different groundwater depths from soil surface (Z, in cm) and one combination of "other" parameters such as soil type, climate, and vegetation. Note that this loss function represents net loss of water from the root zone since it incorporates the effect of capillary upflow, which is a gain to the root zone.

[16] In contrast to the more traditional *Eagleson* [1978] approximation (which we applied in the work by *Vervoort and van der Zee* [2009]), drainage and capillary upflow never occur simultaneously in this function; more specifically, it contains a switching behavior for which the switching point $s_{\lim}$ is dependent on the groundwater depth. In order to separately calculate the capillary upflow U, we have used equation (4) [*Vervoort and van der Zee*, 2008], and the leaching flux has been calculated by using the lower limit of soil saturation (excluding the η parameter) of equation (2). The maximum evapotranspiration $E_{\max}$ has been calculated by using *Teuling and Troch*'s [2005] equation. We checked that the sum of the separate loss function

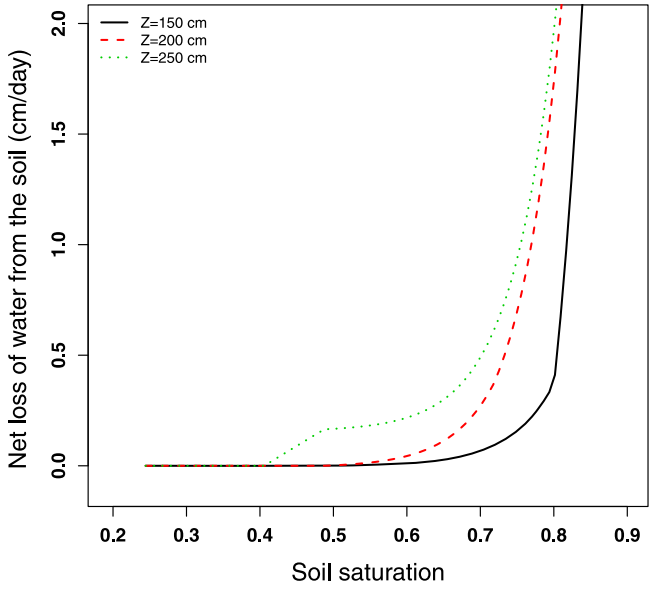

Figure 2. Graphical representation of equation (2) (net loss of water as a function of soil saturation) for sandy clay loam soil (SCL, Table 1) under three different groundwater depths ($Z = 150$ cm, $Z = 200$ cm, and $Z = 250$ cm). $E_{\max} = 0.37$ cm d^{-1}, and vegetation is trees (Table 2).

and combined calculation of the fluxes combined in (2) indeed gave the same result:

$$q_{\text{total}}(s) = \begin{cases} -m_2 & s_{cr} < s \le s^* \\ -m_1\left[1 - e^{\beta(s - s_{\text{lim}})}\right] & s^* < s \le s_{\text{lim}} \end{cases},$$
$$m_2 = \frac{K_s G}{\phi Z r}, \tag{4}$$
$$m_1 = \frac{m_2}{\left[1 - e^{\beta(s^* - s_{\text{lim}})}\right]}.$$

[17] Also in Figure 2, the impact of ET can be seen when the groundwater level is deep and cannot be observed for shallow water tables. For shallow water levels, the effect of ET is not visible because capillary upflow is in balance with ET losses. Basically, the impact of capillary upflow is that at some value of s the total loss (ET $-$ U) from the root zone actually equals zero. The soil will never dry out below this level of soil saturation because at this critical saturation s_{cr} and below, the potential capillary flux is either equal to or larger than the actual evaporation losses, and thus, all evaporation demands can be supplied by the capillary flux. In reality, below s_{cr} the potential capillary upflow will be reduced until capillary upflow matches the actual ET. This also implies that s_{cr} is the minimum soil saturation level that the soil will reach a particular groundwater level, ET demand curve, and soil type, and therefore, these factors depend on s_{cr}. For shallow groundwater tables, s_{cr} is equal to s^*, and for deep groundwater tables, s_{cr} is equal to s_w. As a result, the ET signal is more clearly visible for deep groundwater tables in Figure 2.

[18] The model as formulated in equations (1) and (2) can be solved analytically to give the soil saturation probability density function [*Vervoort and van der Zee*, 2008], but all other salt-related variables and the separate fluxes (i.e., U, L, and ET) must be calculated numerically. In this study, we will concentrate on the situation where the capillary fluxes supply sufficient moisture so $s_{cr} \ge s_w$ and $m_2 > E_w/\phi Z_r$, where E_w is the residual soil evaporation. Strictly speaking, equation (2) only applies in the case that $m_1 < \eta$, which means $s_{cr} < s^*$, or where the capillary fluxes are too small to maintain evapotranspiration at maximum capacity [*Vervoort and van der Zee*, 2008].

[19] A different situation arises for very shallow water tables, where $m_1 > \eta$. In this case, $s_{cr} > s^*$, and equation (2) simplifies to two piecewise linear sections [see *Vervoort and van der Zee*, 2008, equation (11)], which means the capillary fluxes allow evapotranspiration to always be at its maximum capacity and soil water saturation never drops below s^*.

2.2. Salt Transport Equation

[20] Whereas, in general, each of the water fluxes implies salt transport, some of these dominate salt accumulation. Except for special cases such as coastal regions that experience salt spray [*Suweis et al.*, 2010], the salt flux involved with atmospheric deposition and rainfall may be often ignored. Irrigation with water containing salts means salt fluxes at the soil surface are important [*Bresler*, 1981; *Runyan and D'Odorico*, 2010; *Isidoro and Grattan,* 2011], where the use of wastewater for irrigation is a special case [*Jalali et al.*, 2008]. Still, in this paper, we disregard both poor-quality irrigation water and salt deposition via rainfall. Plants may uptake salts, and dicotyledonous halophytic plants and crops may even require some NaCl for optimal growth [*Rozema and Flowers*, 2008; *Flowers and Colmer,* 2008]. However, the mass fluxes involved in salt uptake and removal from the field in harvested products are generally quite limited [*Shani et al.*, 2007]. For the present case, we therefore only consider the salt mass fluxes due to capillary flux from groundwater, which in this study has a constant concentration C_Z (for our reference case equal to 0.02 $\text{mol}_c\ \text{L}^{-1}$, where mol_c is mole charge) and is unaffected by the processes in the root zone, and the leaching toward groundwater of salts that have accumulated in the root zone. We obtain the following balance equation for the salt mass M:

$$\frac{\text{d}M}{\text{d}t} = \phi Z_r \frac{\text{d}sC}{\text{d}t} = U(s)C_Z - L(s)C, \tag{5}$$

where C is the salt concentration in the root zone in $\text{mol}_c\ \text{L}^{-1}$, C_z is the salt concentration of the groundwater at depth Z in $\text{mol}_c\ \text{L}^{-1}$, M is the salt mass in $\text{mol}_c\ \text{m}^{-2}$, and s is the soil saturation. As (5) shows, we disregard chemical interactions such as sorption and precipitation or dissolution [*Shani et al.*, 2007; *van der Zee et al.*, 2010]. Since we focus on easily soluble salts such as NaCl that dominate seawater and are often the most important salts for groundwater [*Appelo and Postma*, 2005], the omission of chemical interactions is appropriate. We recognize that even for sodium, this is an approximation [*Bolt*, 1982; *Kaledhonkar et al.*, 2001; *van der Zee et al.*, 2010]. The coupled equations (1) and (5) are solved numerically to provide root zone saturation, salt mass and concentration, and the contribution of various water and salt fluxes.

[21] The matric potential $h(s)$ of the root zone controls the water fluxes. In the analysis of *Vervoort and van der Zee* [2008], however, the main variable is the soil water saturation s, which is uniquely related to the matric potential. In the present case, besides the matric potential that predominantly reflects capillary forces, the osmotic potential is also important, given the presence of salts. Therefore, we need to combine the matric and osmotic potentials and, following the concept of chemical potential, determine a "virtual" saturation s_v using $s(h)$, which then controls evapotranspiration and capillary and leaching fluxes. Assuming validity of van't Hoff's law, we used a salinity correction based on the additive properties of matric and osmotic potentials [*Bras and Seo*, 1987; *De Jong van Lier et al.*, 2008] even though this convention can be disputed. The osmotic potential follows the van't Hoff's law. Once the ionic components of the salt solution in the root zone is known, $\pi(C)$ is a linear function of the salt concentration C, which can be written as

$$\pi(C) = kC, \tag{6}$$

where π is osmotic potential (MPa), C is the salt concentration expressed as $\text{mol}_c\ \text{L}^{-1}$, and k is a coefficient that includes the effect of temperature, electrolyte properties, and a unit conversion factor, which is equal to 3.6 MPa L mol_c^{-1}. The osmotic potential can subsequently be combined with the *Brooks and Corey* [1966] equation, which describes the matric potential relationship with soil saturation:

$$h(s) = h(1)\left(\frac{s}{s_s}\right)^{-b}, \tag{7}$$

where $h(1)$ is the saturated soil matrix potential (MPa), b is a parameter related to conductivity and tortuosity (pore size distribution index and related to the previously mentioned parameter β), and s_s is soil saturation ($s_s = 1$). We can combine (6) and (7) and rearrange to obtain the virtual saturation s_v [*Bras and Seo*, 1987]:

$$s_v = s_s h(1)^{1/b} \left[h(1) \left(\frac{s}{s_s} \right)^{-b} + kC \right]^{-1/b}. \quad (8)$$

The resulting virtual soil saturation is the soil saturation available to plants taking into account both matric and osmotic effects.

2.3. Calculations

[22] Numerical simulations were based on a similar parameterization to the one by *Vervoort and van der Zee* [2008] (Tables 1 and 2) and therefore allow for comparison with their results (which were focused towards analytical probability density functions (pdfs) of the root zone water saturation).

[23] Different Australian soils were considered where the porosity ϕ was set equal to θ_s as estimated with the van Genuchten pedotransfer functions in Neurotheta [*Minasny and McBratney*, 2002]. Some representative climate parameters were calculated from long-term rainfall data for several locations in Australia [*Vervoort and van der Zee*, 2008], and this defined the range of possible values for α and λ used in this paper. The climate is characterized by $\alpha\lambda/E_{\max}$, which gives dimensionless values of 0.89, 1.35, and 1.89 for dry, semiarid, and wet climates, respectively. These dimensionless values are calculated on the basis of input values of α and λ used in the rainfall model. Maximum evaporation $E_{\max}$ was calculated using the *Teuling and Troch* [2005] equation, and values are listed in Table 3.

[24] In the model, we assume that only part of the real rainfall may enter the root zone. Note that real rainfall is not exactly the same as rainfall input (input values of $\alpha\lambda$) because the rainfall model generates relatively less rainfall than the rainfall input taking into account interception. The modeled rainfall is also called achieved rainfall or actual input. If the amount of rainfall is greater than the current storage capacity, which is related with $1 - s$, then the excess rainfall is lost because of runoff, and the remaining rainfall enters the system for soil saturation calculations (following the original model by *Laio et al.* [2001]). Surface runoff due to a limited infiltration capacity could also be considered [*Appels et al.*, 2011] but will not affect the main message of our paper, especially for larger root zone thicknesses. Model calculations were done for a simulated time of 100 years, as this was needed to reach a steady state salt concentration. In view of the boundary conditions that change with time, this refers to a steady state in the trend of erratically fluctuating state variables, such as saturation, salt mass, concentration, and various fluxes. In our analysis, the first simulated year was ignored as a warm-up period, and results were therefore obtained for a 99 year period, and means were stabilized during this period as shown in Table 4. For the period after the initial conditions had decayed, long-term (pseudosteady state) statistics were calculated. Typically, statistics and pdfs required computed times larger than 20 years. We determined these properties for the period ranging from about year 30 to year 100, but for comparison with the analytical solution for saturation in Figure 3, about a threefold larger period was considered to more accurately determine the pdfs. All the values under each climate are calculated for one realization of rainfall function as different realizations only cause small variations in the numerical outcomes.

Table 1. Soil Properties Used in the Simulations[a]

Soil Type	Porosity ϕ	K_s (cm d^{-1})	b	$\bar{\Psi}_s$ (MPa)	Ψ_{s,s_h} (MPa)	S_{fc}
Heavy clay	0.45	2.82	16.2	-1.4×10^{-3}	-10	0.88
Medium clay	0.44	6.04	13.5	-1.7×10^{-3}	-10	0.87
Light medium clay	0.42	3.51	13.5	-1.5×10^{-3}	-10	0.86
Sandy clay loam	0.37	52.08	6.41	-1.2×10^{-3}	-10	0.73
Loamy sand	0.37	175.3	4.52	-0.7×10^{-3}	-10	0.57

[a]Soil hydraulic data are based on standard Australian soils in Neurotheta [*Minasny and McBratney*, 2002].

Table 2. Vegetation Properties Used in the Simulations Following *Porporato et al.* [2001]

	Trees
Zr (cm)	100
Δ (cm)	0.2
$E_{\max}$ (cm d^{-1})	0.5
E_w (cm d^{-1})	0.01
ψ_{s,s^*} (MPa)	-0.12
$\psi_{s,sw}$ (MPa)	-2.5
Leaf area index ξ	2.5[a]

[a]From *Whitehead and Beadle* [2004].

3. Results

3.1. Comparison of Analytical and Numerical pdfs of Soil Saturation

[25] For the water balance, only one factor differs compared with the situation considered by *Vervoort and van der Zee* [2008], which is the effect of the osmotic potential. In Figure 3, we show the pdfs of root zone water saturation for the cases with and without accounting for osmotic effects for three groundwater depths ($Z = 150$ cm, $Z = 250$ cm, and $Z = 350$ cm) under a dry climate ($\alpha\lambda/E_{\max} = 0.89$) and a wet climate ($\alpha\lambda/E_{\max} = 1.89$). The actually achieved rainfall was 0.219 and 0.426 cm d^{-1}, respectively (Table 4). First, we compare the numerically determined pdfs for different climates and groundwater levels Z with the analytical results without osmotic effect from *Vervoort and van der Zee* [2008]. This comparison was not done in that paper, and in fact, we found little evidence of the accuracy of such

Table 3. Climate Properties Used in Simulations[a]

Climate	α (cm event^{-1})	λ (events d^{-1})	Modeled Rainfall Input (cm d^{-1})	$E_{\max}$ (cm d^{-1})
Dry	1.1	0.3	0.33	0.37
Semiarid	1.25	0.4	0.5	0.37
Wet	1.4	0.5	0.7	0.37

[a]These properties were calculated using the methods described by *Rodriguez-Iturbe et al.* [1984].

Table 4. Long-Term Average Values of Salt Concentration, Soil Saturation, Salt Mass, Capillary Flux, Leaching Flux, Evapotranspiration (Soil Saturation), Change in Soil Saturation Storage, and Runoff for Six Groundwater Depths and Three Climates[a]

Groundwater Depth (cm)	Salt Concentration C ($mol_c\ L^{-1}$)	Relative Saturation s	Salt Mass ($mol_c\ m^{-2}$)	Capillary Flux ($cm\ d^{-1}$)	Leaching Flux ($cm\ d^{-1}$)	ET (s) ($cm\ d^{-1}$)	dS ($\times 10^{-5}\ cm\ d^{-1}$)	Runoff ($\times 10^{-5}\ cm\ d^{-1}$)	Actual Input ($cm\ d^{-1}$)	Numerical Error ($\times 10^{-5}\ cm\ d^{-1}$)
150	0.054	0.771	15.220	−0.137	0.058	0.298	−3.040	8.180	0.219	−0.11
200	0.056	0.697	14.423	−0.117	0.048	0.288	−3.270	0.000	0.219	−0.135
250	0.062	0.643	14.681	−0.083	0.033	0.269	1.450	0.000	0.219	−0.018
300	0.066	0.592	14.342	−0.055	0.022	0.252	8.510	0.000	0.219	−0.086
350	0.065	0.552	13.157	−0.037	0.015	0.240	8.370	0.000	0.219	−0.109
400	0.061	0.524	11.675	−0.026	0.012	0.233	6.490	0.000	0.219	−0.124
150	0.034	0.772	9.741	−0.134	0.090	0.354	−1.250	31.900	0.310	−0.516
200	0.035	0.700	9.050	−0.112	0.076	0.347	−1.090	5.200	0.310	−0.524
250	0.037	0.647	8.701	−0.078	0.054	0.334	−0.786	1.830	0.310	−0.497
300	0.036	0.600	7.871	−0.050	0.038	0.322	0.671	0.910	0.310	−0.536
350	0.033	0.567	6.761	−0.033	0.029	0.314	−0.396	0.174	0.310	−0.554
400	0.028	0.543	5.677	−0.023	0.023	0.309	−1.800	0.000	0.310	−0.553
150	0.015	0.780	4.437	−0.107	0.161	0.371	−1.370	53.500	0.426	2.15
200	0.015	0.711	3.843	−0.084	0.138	0.371	−1.340	2.010	0.426	2.12
250	0.013	0.666	3.216	−0.055	0.109	0.371	−4.530	0.000	0.426	1.95
300	0.010	0.631	2.426	−0.033	0.089	0.369	−8.150	0.000	0.426	1.8
350	0.008	0.608	1.710	−0.020	0.080	0.365	−10.500	0.000	0.426	1.76
400	0.005	0.595	1.184	−0.013	0.076	0.363	−11.900	0.000	0.426	1.74

[a]The actual input represents the precipitation (P) generated by the Poisson model using the standard α and λ parameters (Table 3), taking into account interception [*Laio et al.*, 2001]. The eleventh column represents the water balance closure error in the model for the 99 year simulations presented here.

analytical solutions in the literature cited in that paper. For the comparison, we used the numerically achieved values of α and λ. The general agreement between numerical and analytical pdfs is quite good. The numerical pdfs (for all climates) slightly underestimate the analytical pdfs of soil saturation, especially for deeper groundwater levels, where they shift somewhat to the dry end compared to the analytical solutions. The first main reason for this difference is the bias caused by the small sample on which the pdfs of the numerical results are based. This bias decreases as the sampling period increases and the moments stabilize. The second reason is that the actually achieved rainfall taking into account interception from the rainfall model is relatively less than the input rainfall, and this error increases as the climates switches from dry to wet climate. The numerical results of Figure 3 are based on 100K day simulation, but still demonstrate some differences between the analytical and numerical results that are due to underprediction of rainfall from the rainfall model.

[26] Figure 3 also reveals that the osmotic effect moves saturations to higher values. This is logical, as the salt effects decrease evapotranspiration losses as well as leaching losses, whereas they increase capillary influxes (hygroscopic effect). On average, larger s values favor larger leaching losses, but apparently this feedback is limited, particularly for deeper groundwater. Still, as leaching prevents saturation from moving much past $s_{\lim}$ (see Figure 3), the pdfs become a bit more peaked.

3.2. Salt Mass and the Related pdf

[27] For a sandy clay loam soil type (SCL) and a root zone thickness Z_r of 100 cm, the evolution of the salt mass and the related pdfs are shown in Figure 4. The temporal development of salt mass is shown for three climates (dry ($\alpha\lambda/E_{\max} = 0.89$), semiarid ($\alpha\lambda/E_{\max} = 1.35$), and wet climates ($\alpha\lambda/E_{\max} = 1.89$)) and three groundwater depths ($Z = 150$ cm, $Z = 200$ cm, and $Z = 250$ cm). The primary results of the numerical calculations are the patterns of salt mass as a function of time, but it is easier to observe the differences between different groundwater levels and climate from the pdfs of salt mass. These are shown for six groundwater depths (Z = 150–400 cm in 50 cm increments). The dynamics of the salt mass lead to three major observations: (1) A wetter climate leads to a smaller salt mass in the root zone. (2) The salt mass is larger for a shallow groundwater level than for a deeper groundwater level. (3) In relative terms, the variability between groundwater depths is greater for the wet climate; however, in absolute terms the opposite is true: the means differ by 5 $mol_c\ m^{-2}$ in the dry case but only by 3 $mol_c\ m^{-2}$ for the wet case.

3.3. Salt Concentration and the Related pdf

[28] For the same combinations as in section 3.2 (and Figure 4), the results are shown in Figure 5 as the salt concentration and the related pdf. The behavior of salt concentration leads to three major observations: (1) For a wet climate, the salt concentration is smaller than for the other climates. (2) The largest concentrations are found for a dry climate, with a maximum for groundwater levels of about 3 m below the soil surface (i.e., 2 m below the 100 cm thick root zone). (3) For a wet climate, the salt concentration has a maximum at shallower groundwater level, whereas for

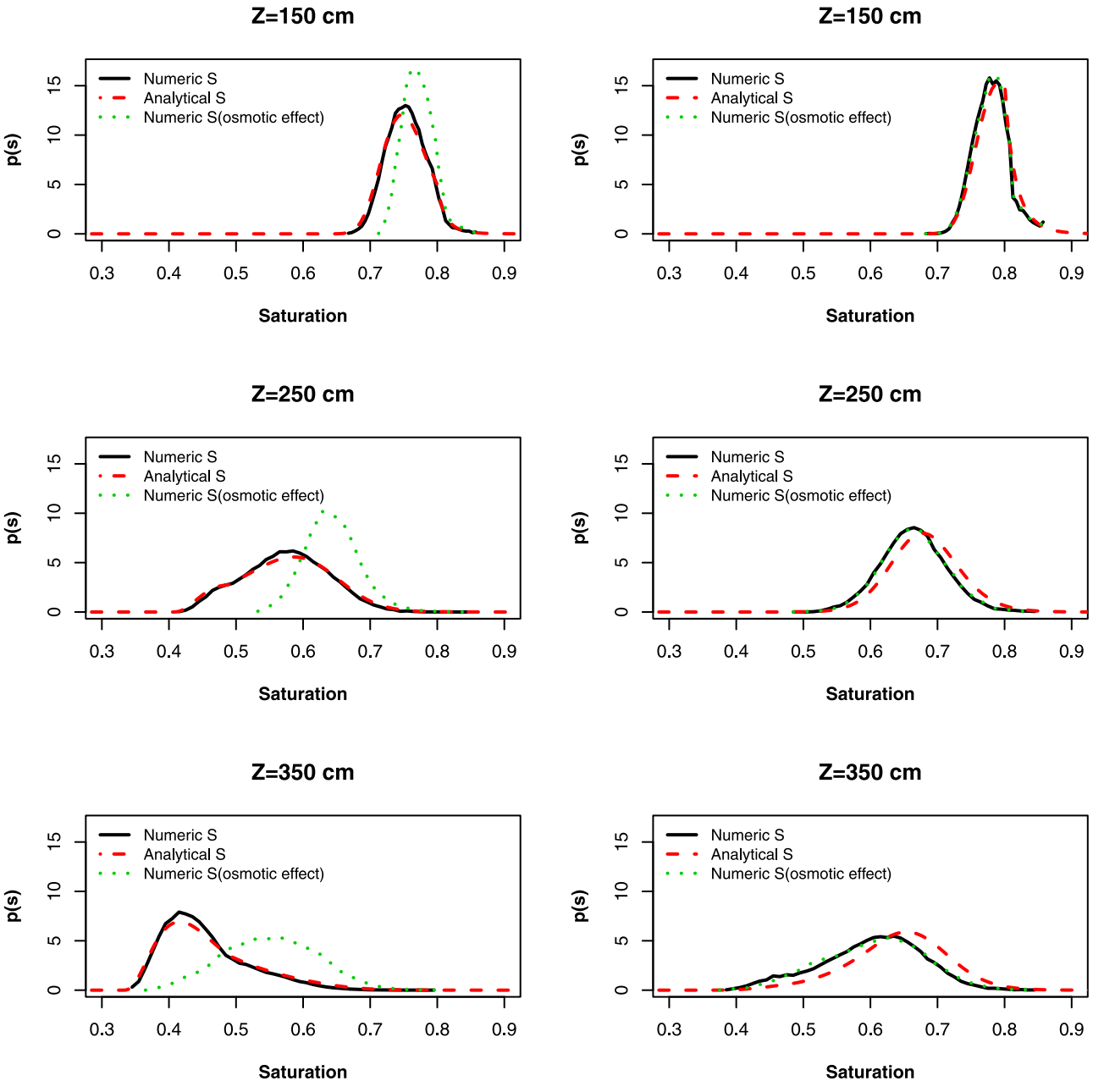

Figure 3. Probability density function (pdfs) of numerical saturation without osmotic effects, analytical saturation, and the numerical saturation with osmotic effects for (left) a dry climate ($\alpha\lambda/E_{\max} = 0.89$) and (right) a wet climate ($\alpha\lambda/E_{\max} = 0.89$ cm d^{-1}) under three groundwater depths ($Z = 150$ cm, $Z = 250$ cm, and $Z = 350$ cm). The vegetation is trees (Table 2), and the soil is a SCL (Table 1).

the other climates, the largest concentrations are found for intermediate groundwater depths. This pattern is consistent with the patterns for the salt mass. That the salt concentration is not necessarily dependent on the groundwater depth in a monotonous way is indicative of the counteracting effects of rainfall and capillary upflow.

3.4. Effect of Varying Soil Type

[29] Besides different climates and groundwater levels, parameters such as soil type, root zone depth, and groundwater salinity affect the concentration in the root zone. For this reason, we considered different soil types listed in Table 1, where we observe that these soils differ in several hydraulic parameters, but mainly in the hydraulic conductivity. The long-term average root zone concentration was calculated and is presented as a function of the hydraulic conductivity of the five soils in Figure 6. For all three climates and larger Z, the average root zone concentration increases as the hydraulic conductivity increases, with one exception (loamy sand (LS), which has the largest hydraulic conductivity). However, as the climate becomes drier, a reversal is seen for shallow groundwater: the average root zone concentration increases as hydraulic conductivity decreases. In interpreting Figure 6, it is necessary to appreciate that the above

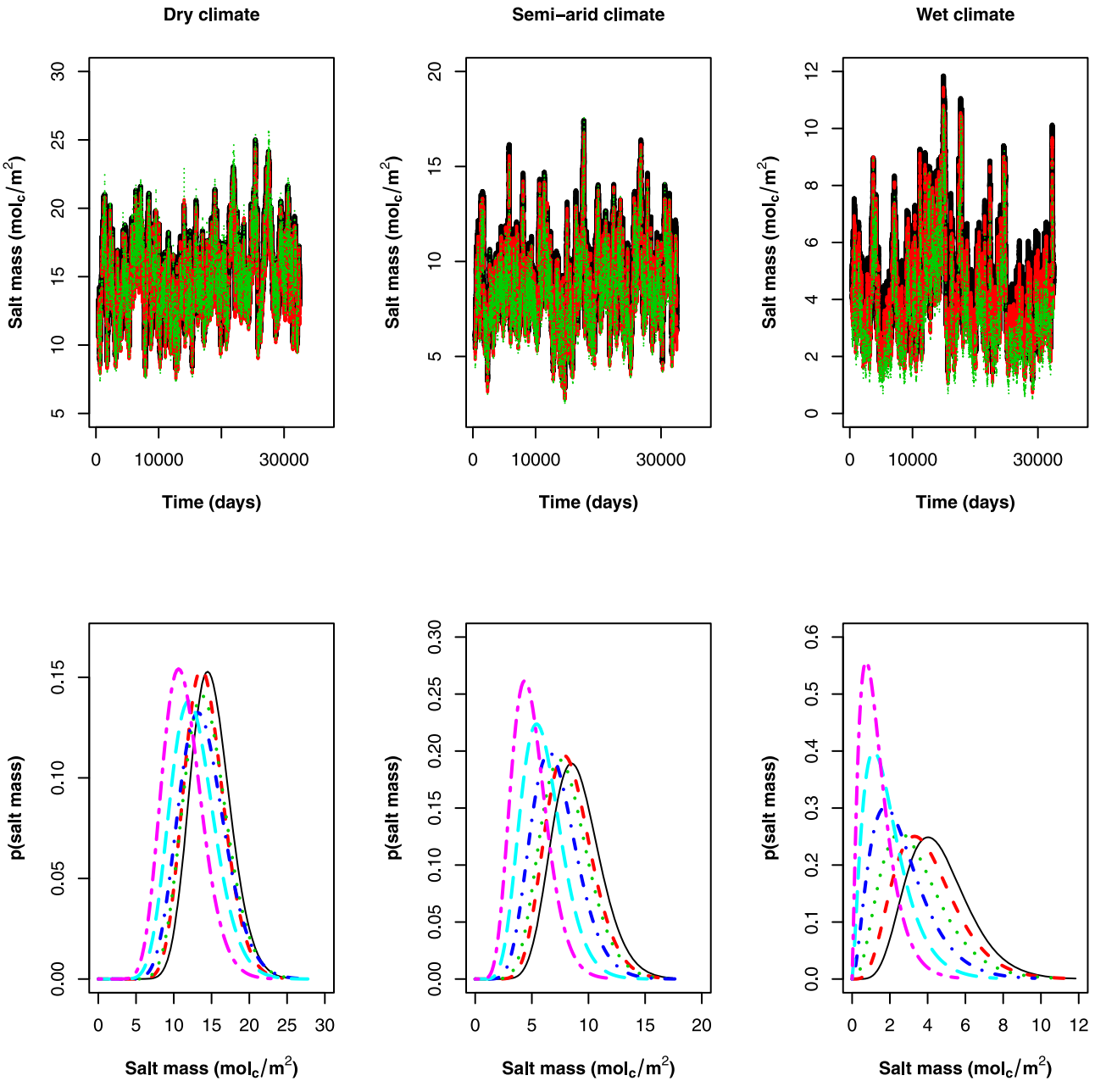

Figure 4. Development of the salt mass during 99 years for three different groundwater depths ($Z = 150$ cm (black), $Z = 200$ cm (red), and $Z = 250$ cm (green)) below the soil surface. The pdfs of salt mass are shown for six groundwater depths ($Z = 150$ cm (black solid line), $Z = 200$ cm (red dashed line), $Z = 250$ cm (green dotted line), $Z = 300$ cm (blue dashed-dotted line), $Z = 350$ cm (turquoise dashed line), and $Z = 400$ cm (pink dashed-dotted line)). Both salt mass and related pdfs are plotted for three different climates (dry climate $(\alpha\lambda/E_{\max} = 0.89)$, semiarid climate $(\alpha\lambda/E_{\max} = 1.35)$, and wet climate $(\alpha\lambda/E_{\max} = 0.89)$). The vegetation is trees (Table 2), and the soil is a SCL (Table 1).

observations are all based on long-term average concentrations. Particularly for the leaching process under dry conditions, short-term, high-intensity showers may control leaching, rather than the average, and may be dominant in how the concentration level develops.

3.5. Effect of Root Zone Thickness and Groundwater Salinity

[30] Besides the differences between soil type, groundwater level, and climate (evapotranspiration demand and rainfall), vegetation is a further important aspect to salt accumulation. A range of properties of vegetation can be important, e.g., those of Table 2. To focus on the system behavior, we varied the root zone thickness Z_r and the groundwater salinity (i.e., the impact of osmotic stress). To separate the effect of root zone thickness from groundwater depth, we varied Z_r for different distances of capillary upflow: $Z - Z_r$ [*Vervoort and van der Zee*, 2008, 2009]. In Figure 7, we show the results of varying root zone thickness for a wet climate and for a dry climate.

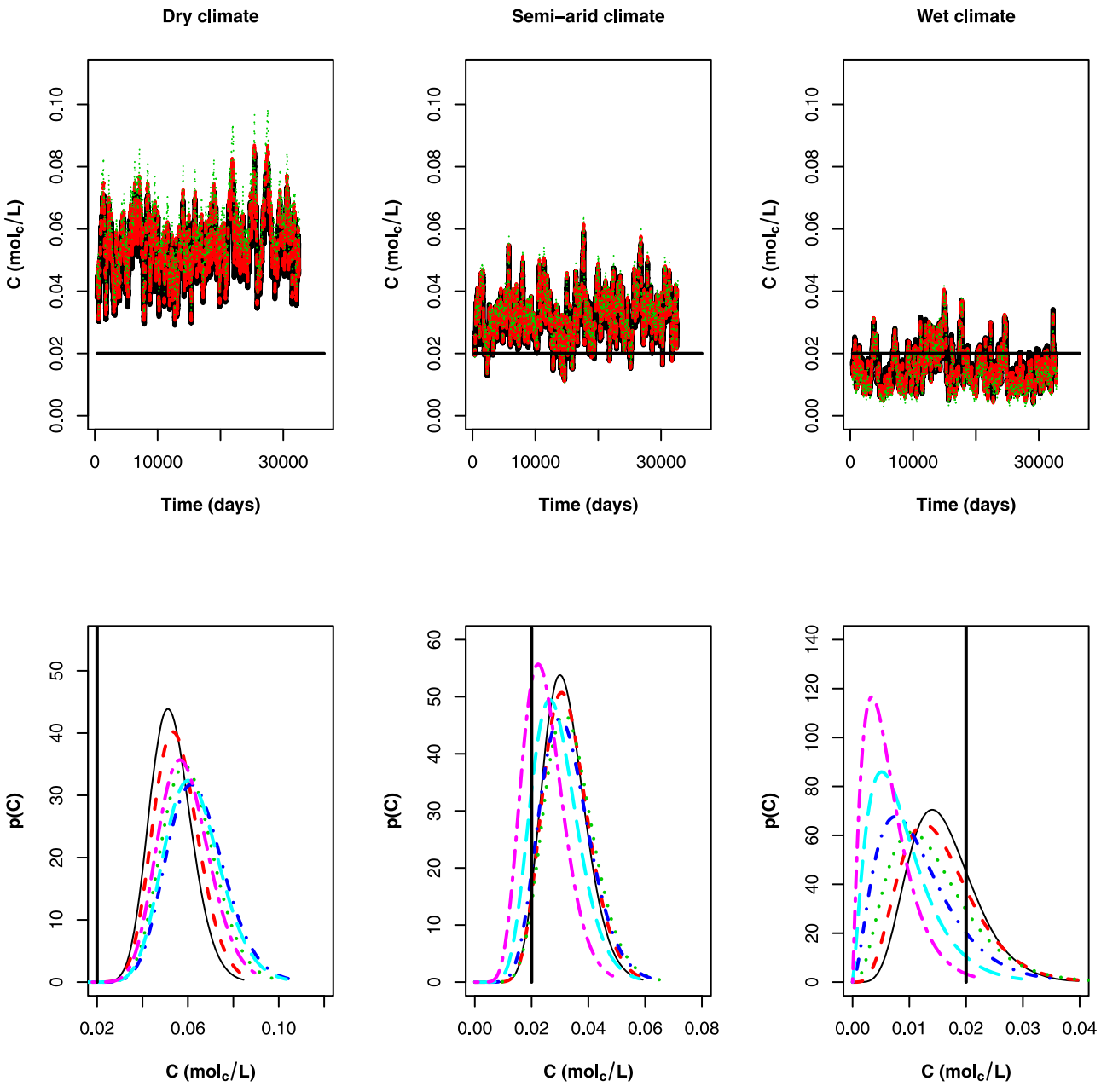

Figure 5. Development of the salt concentration during 99 years for three different groundwater depths ($Z = 150$ cm (black), $Z = 200$ cm (red), and $Z = 250$ cm (green)) below the soil surface. The pdfs of salt concentration are shown for six different groundwater depths ($Z = 150$ cm (black solid line), $Z = 200$ cm (red dashed line), $Z = 250$ cm (green dotted line), $Z = 300$ cm (blue dashed-dotted line), $Z = 350$ cm (turquoise dashed line), and $Z = 400$ cm (pink dashed-dotted line)). The horizontal and vertical thick solid black lines show the groundwater salt concentration ($C_z = 0.02$ mol$_c$ L^{-1}). The vegetation is trees (Table 2), and the soil is a SCL (Table 1). Other conditions are as in Figure 4.

[31] The concentration of salt in the groundwater C_Z was varied as follows: $C_Z = 0.02$ mol$_c$ L^{-1} (reference), 0.01 mol$_c$ L^{-1}, and 0.04 mol$_c$ L^{-1} for a dry climate, and for a wet climate. For the wet climate, the average salt concentration in the root zone decreases monotonically with increasing $Z - Z_r$ (distance of groundwater to below root zone), which has been observed already in Figure 5. As Figure 7 indicates, such a monotonic decrease does not occur for the dry climate.

[32] Considering that for Figure 7 the root zone thickness decreases by a factor of 4, whereas the involved relative concentration change increases by a factor of 1.5 for the wet climate, this indicates that root zone thickness has a modest effect. For the dry climate, the relationship between C/C_Z and the distance between root zone and groundwater is nonmonotonic, and the impact of root zone thickness is larger than for the wet climate. Larger salinities are found as root zone thickness increases (as opposed to the wet

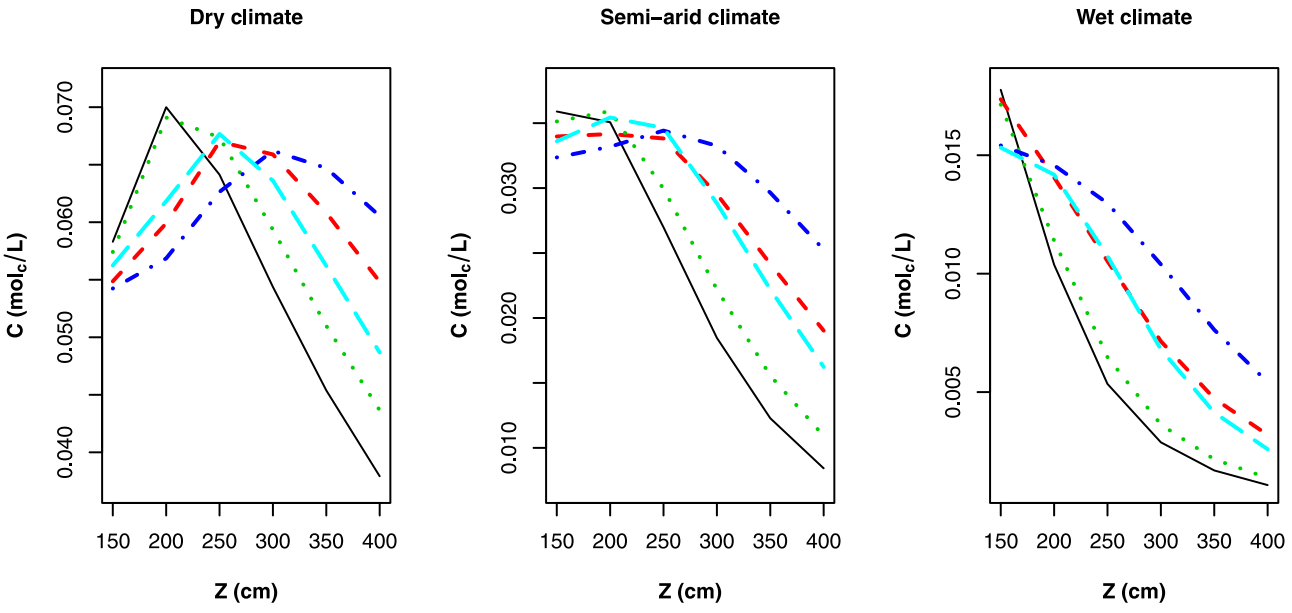

Figure 6. Long-term average salt concentration as a function of six different groundwater depths (Z = 150 cm, Z = 200 cm, Z = 250 cm, Z = 300 cm, Z = 350 cm, and Z = 400 cm) under different soil types: heavy clay (black solid line), medium clay (red dashed line), light medium clay (green dotted line), sandy clay loam (blue dashed-dotted line), and loamy sandy soil (turquoise dashed line) (Table 1). Other conditions are as in Figure 4.

climate), and in particular, the impact of salinity of groundwater is much larger than for the wet climate.

3.6. Mapping the Root Zone Salinity as a Function of Climate Parameters

[33] Practically, it is of interest to recognize which combination of factors lead to adverse salinity levels in the root zone. Therefore, we map the combinations of two climate parameters (α and λ) that result in a particular salinity in Figure 8. For a range of rainfall parameters ($\alpha = 1.1 - 1.4$ cm event^{-1}, $\lambda = 0.3 - 0.5$ event d^{-1}), the SCL soil, root zone thickness (Z_r = 100 cm), and a groundwater level equal to Z = 300 cm, we calculated the resulting (99 year average root zone) salt concentrations of Figure 8a. This range of rainfall parameters covers the three values of $\alpha\lambda$ (climate parameters) that have so far been considered in this paper (with $\alpha\lambda$ ranging from 0.33 to 0.70 cm d^{-1}; Table 3).

[34] Since the critical groundwater depth Z (where salt concentration is maximum) is 300 cm for sandy clay loam soil (Z = 300 cm, $\alpha\lambda$ (actual input) = 0.219 cm d^{-1} in Table 4), we have selected this groundwater depth in order to visualize the effect of small and large frequent events on the range of root zone salt accumulation. The range of numerically obtained salt concentrations in the root zone as shown in Figure 8a exceeds the critical value (0.04 mol$_c$ L^{-1}) where production of sensitive plants decreases. For these conditions, concentrations increase as the climate becomes drier, which is in agreement with Figure 4. In addition, rainfall frequency affects the salinity that will develop. As rainfall occurs less frequently, salinity increases to greater levels.

[35] At a first glance, frequency seems to have a lesser effect on salinity than other parameters like rainfall quantity, root zone thickness, and groundwater depth. Therefore, the results of Figure 8b are also sensitive to other parameterizations. For instance, we conducted calculations that are parameterized for a wheat crop, with Z_r = 65 cm and a matric potential where transpiration becomes limited that is representative for wheat ($\psi_{s,s^*} = -0.09$ MPa [*Kroes et al.*, 2008]), a groundwater level of Z = 200 cm, and a range of α (1–1.2 cm event^{-1}) and λ (0.1–0.2 event d^{-1}) parameters.

[36] The results shown in Figure 8b indicate that the average salt concentrations are greater than for Figure 8a and are also comparable with the critical levels derived from *Richards et al.* [1954]. In addition, the contour lines of average salt concentration are almost vertically oriented in Figures 8a and 8b. As the climate becomes strongly drier, the salt concentration increases, and subsequently, contour lines become almost horizontally oriented (not shown). In these severe conditions, average salt concentration exceeds the critical value (0.08 mol$_c$ L^{-1}) where only tolerant plants can show good primary production.

3.7. Analytical Approximation

[37] The erratic patterns of concentration as a function of time are caused by the Poisson rainfall and can be conceived as resulting from an input of salt mass due to capillary flow from groundwater and the leaching due to rainfall. Assuming constant salt inputs Y in terms of concentration units (i.e., input of mass of salt divided by root zone water volume) occurring instantaneously with a recursion time of Δt and followed by periods of leaching, with a leaching flow rate equal to j_l, a root zone water volume equal to V, and a number of years equal to n, the maximum concentrations of the developing sawtooth pattern can be approximated by [*van der Zee et al.*, 2010]

$$C_{\max} = Y\left\{\frac{1-\left[\exp\left(-\frac{j_l}{V}\Delta t\right)\right]^n}{1-\exp\left(-\frac{j_l}{V}\Delta t\right)}\right\}. \quad (9)$$

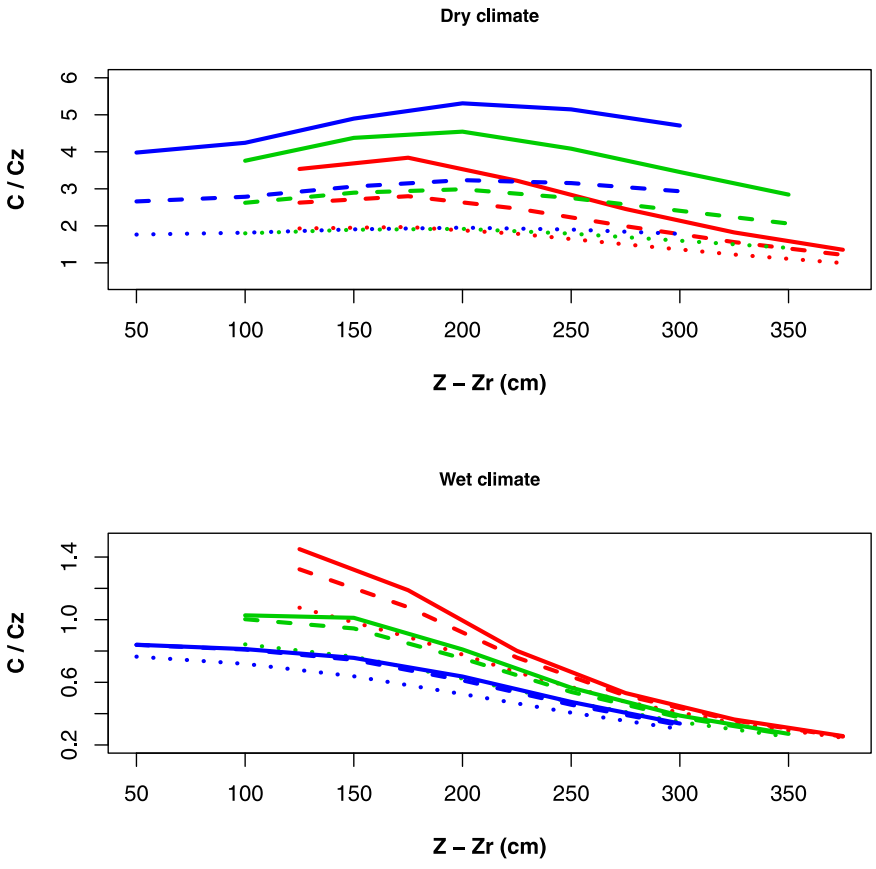

Figure 7. The long-term average salt concentration as a function of $Z - Z_r$ for different root zone thickness (red, $Z_r = 25$ cm; green, $Z_r = 50$ cm; blue, $Z_r = 100$ cm) under different groundwater salinities (solid lines, $C_z = 0.01$ mol$_c$ L^{-1}; dashed lines, $C_z = 0.02$ mol$_c$ L^{-1}; dotted lines, $C_z = 0.04$ mol$_c$ L^{-1}) and two climates (dry climate $(\alpha\lambda/E_{max} = 0.89)$ and wet climate $(\alpha\lambda/E_{max} = 0.89)$). The vegetation is trees (Table 2), and the soil is a SCL (Table 1).

The minimum salt concentration is calculated by subtracting the salt input Y from the C_{max} value:

$$C_{min}(n) = C_{max}(n+1) - Y. \tag{10}$$

To check whether this simple approach captures the dynamics of the random patterns presented earlier, we use the annual averages of the numerically determined drainage rates and capillary flux to approximate the water flux, j_l (cm yr^{-1}), and capillary flux (cm yr^{-1}), and with the long-term averaged water saturation and the root zone porosity ϕ, we estimate the root zone water volume as $V = \phi Z_r \langle s \rangle$. The recursion time is set equal to 1 year, and the applied salt mass (in concentration equivalents) is equal to Y(mol$_c$ L^{-1}) $= (\langle U \rangle C_Z)/(\phi Z_r \langle s \rangle)$, where the mean capillary flux and water saturation were again taken from the numerical calculations. In all cases, we used averages for simulation times exceeding 10,000 days. Using equations (9) and (10), we calculated the maximum concentrations and the minimum concentrations for the erratic patterns of salt concentration (Figure 9). Whereas for the dry climate the agreement is not good, particularly for deeper groundwater levels (not shown), for the semiarid (Figure 9) and wet climate (not shown), the agreement is reasonable to good for the time period exceeding 10,000 days, and the average of minimum and maximum concentrations gives a good impression of the long-term mean C value.

[38] In equation (9), the term to the power n decays rapidly. Therefore, we can simplify this equation further by ignoring this decaying term to obtain

$$C_{max} = Y\left[1 - \exp\left(-\frac{j_l}{V}\Delta t\right)\right]^{-1} = YX. \tag{11}$$

We can approximate C_{max} with the 84th percentile C value in the numerical concentration pdfs, and

$$YX = \frac{\langle U \rangle C_Z}{\phi Z_r \langle s \rangle} X, \quad X = \left[1 - \exp\left(-\frac{j_l}{V}\Delta t\right)\right]^{-1}, \quad \frac{j_l}{V} = \frac{\langle L \rangle}{\phi Z_r \langle s \rangle}.$$

[39] For five soil types and different groundwater depths and climates, we calculated YX and plotted the approximated maximum concentration as a function of this product in Figure 10. Considering the coarse approximation, the agreement is quite good. As the climate becomes wetter, soil saturation, evapotranspiration, and leaching increase, but the capillary upflow decreases.

[40] Since salt transport is caused by the capillary flux, less salt enters the root zone for a wetter climate, and this

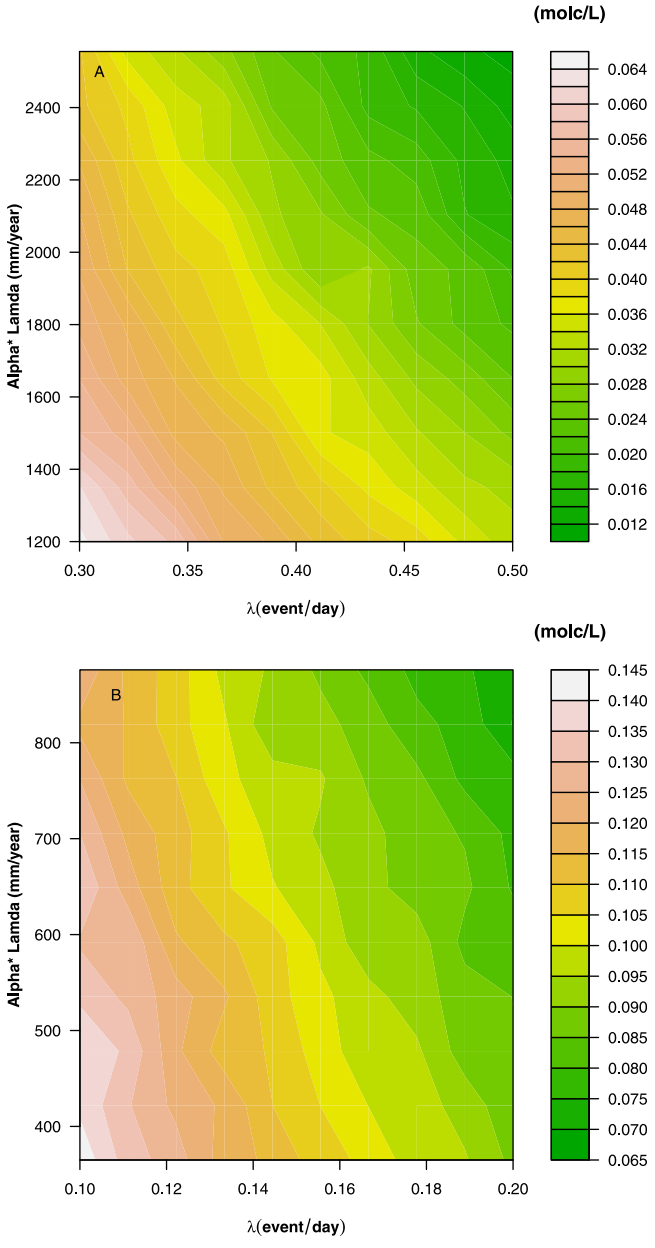

Figure 8. (a) Contour lines of average salt concentration ($\mathrm{mol_c\ L^{-1}}$) as a function of rainfall ($\alpha\lambda$, mm $\mathrm{yr^{-1}}$) and rainfall frequency ($\lambda = 0.3 - 0.5$ event $\mathrm{d^{-1}}$). The groundwater depth Z is 300 cm, and vegetation is trees (Table 2). (b) Contour lines of average salt concentration ($\mathrm{mol_c\ L^{-1}}$) as a function of rainfall ($\alpha\lambda$, mm $\mathrm{yr^{-1}}$) and rainfall frequency ($\lambda = 0.1 - 0.2$ event $\mathrm{d^{-1}}$). The groundwater depth Z is 200 cm, and $Z_r = 65$ cm. The vegetation is a wheat crop (except for the root zone depth and $\psi_{s,s^*} = -0.09$ MPa, all parameters are from Table 2). The soil is a SCL (Table 1).

leads to smaller values of $C_{\max}$. Therefore, the $C_{\max}$ values for a wet climate are small and are in the bottom left corner of Figure 10, and for a dry climate they are relatively large. An even coarser approximation is gained by directly comparing the capillary flux U with the leaching flux L. Although these fluxes vary as a function of time, on average, if U is larger than L, it is probable that the concentration in the root zone becomes larger than in the groundwater, whereas if $U < L$, it is likely that salts enter the root zone but are flushed effectively. Hence, in the latter case, concentrations in the root zone remain below C_z (not shown).

4. Discussion

[41] In Figure 3, the pdf of water saturation of the root zone is shown for dry and wet climates. Of interest is that for the wet climate, the pdf including osmotic effects is not much different from those where these effects are ignored. Quite different is the case for the dry climate, where osmotic effects have a major impact on the wetness of soil. Not shown is the pdf for the semiarid climate, but there, osmotic effects are still minor and only slightly larger than for the wet climate. Considering (Figure 5) that long-term average root zone salinities change from wet to dry, from about 0.01 to 0.03 to 0.06 $\mathrm{mol_c\ L^{-1}}$, respectively, it is clear that osmotic effects for the present parameterization may affect the water and salt balances only if concentrations exceed approximately 0.04 $\mathrm{mol_c\ L^{-1}}$.

[42] The salt concentration and salt mass trajectories through time are quite erratic, and where a long-term trend is absent or insignificant, the short-term fluctuations easily cover 50% of the concentration range and even more for the range of salt mass, for each of the climates considered.

[43] To appreciate the effects of two dominant factors, i.e., climate and groundwater depth Z, the probability density functions of salt mass and salt concentration enable a better comparison than the trajectories. For salt mass, the trends are quite simple: salt mass increases as the climate becomes drier and as the depth to groundwater decreases. Both tendencies can be readily understood by considering that as climate becomes drier, root zone water used for evapotranspiration is replenished by brackish water capillary upflow from groundwater, whereas leaching of salt decreases. As groundwater becomes shallower, capillary upflow increases, and salt concentration in the root zone decreases because of the dilution effect, and this dilution effect decreases with the increase of groundwater depth. Therefore, salt concentration is maximum at intermediate groundwater level. Furthermore, as the climate switches from wet to dry, the shift of the pdf of salt mass to the right becomes gradually smaller. Relatively speaking, the shift is largest for the wet climate, which is due to rainfall surplus (Table 4: $P - \mathrm{ET} - R$, where R is runoff). However, for the considered cases the absolute shift of the pdf is relatively constant for all climates (about 4–5 $\mathrm{mol_c\ m^{-2}}$).

[44] For concentration, which is the result of combining the pdfs of salt mass and water storage in the root zone, the shift of the pdf cannot be related to climate and groundwater level quite so easily. The reason is that for the dry and semiarid climates, the pdf shifts more to larger concentrations for the groundwater depths of 300 and 250 cm; that is, the distance between groundwater and the root zone has a nonmonotonous impact on the long-term average root zone concentration.

[45] This more complex behavior than for salt mass must be due to counteracting processes, and two logical candidates are (1) leaching and (2) dilution. Leaching removes salts that have accumulated in the root zone, and the condition necessary for this to happen is a sufficiently large

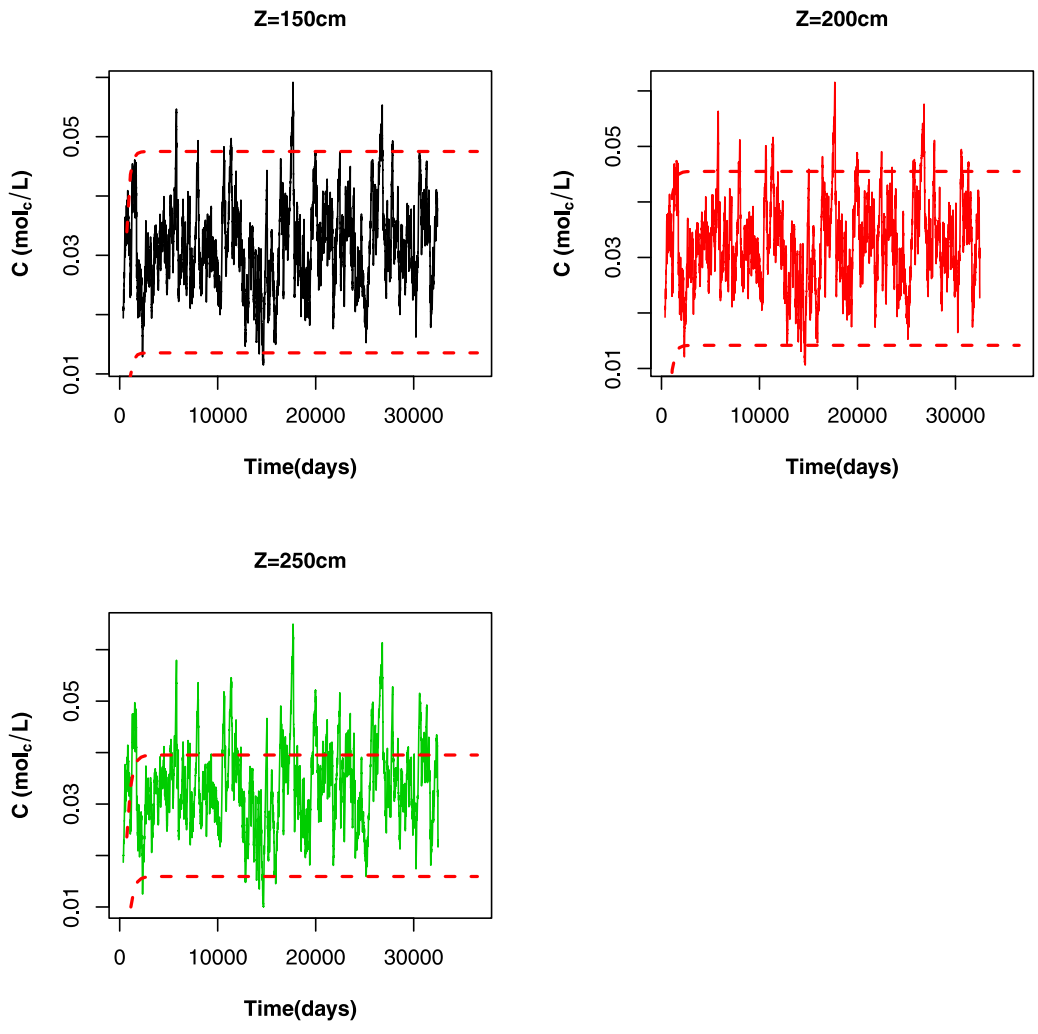

Figure 9. Comparison of long-term concentrations with analytical approximation (C_{max} and C_{min}) for semiarid climate ($\alpha\lambda/E_{max} = 1.35$). The vegetation is trees (Table 2), and the soil is SCL (Table 1).

amount of rainfall that exceeds the available (unused) water storage capacity. Hence, wet conditions due to antecedent rainfall or close proximity of groundwater favor leaching under modest rainfall quantities. A thin root zone also favors leaching, as it implies a small water storage capacity of this zone.

[46] For the wet climate, the frequent rainfall leads to a pdf of water saturation at the wet end, which is quite symmetrical for all groundwater depths (only shown for three groundwater depths in Figure 3). This leads to pdfs of salt mass and concentration that are not much different in shape and that show the same sequence: a shift to the higher values as groundwater is shallower and root zone conditions are wetter. For the dry climate, the water saturation pdf (including osmotic effects) has shifted to smaller saturations for all groundwater depths, and as groundwater levels are deeper, the pdf of saturation is centered around smaller s values, with a few excursions to larger s values. The salt mass pdfs for the dry climate and shallow groundwater levels almost collapse, but the water stored in the root zone decreases rapidly as groundwater levels drop, which causes larger concentrations. For levels of 350–400 cm, the water saturation does not change appreciably compared to 250–300 cm, yet salt mass does, and this is reflected by the pdf of the concentration that has shifted to largest values for the intermediate 250–300 cm groundwater levels. The semiarid climate also shows this nonmonotone behavior of the pdf of salt concentration, though less distinctly than the dry climate.

[47] For the wet climate, groundwater with a salinity of 0.02 mol$_c$ L^{-1} enters the root zone and is diluted by mixing with infiltrating rain water. Despite fluctuations over the years, salt inputs from below are on the longer term balanced by salts that are leached in a volume of water that is larger than capillary upflowing water and a concentration that is less than that of groundwater. Whereas leaching can explain the salt accumulation for the wet climate, for the dry climate, little water leaching occurs as there is a rainfall deficit on average. The numerical results indicate that on average, the capillary upflow rate for the dry climate is larger than the leaching rate, yet over the long term, salt fluxes balance. For a groundwater salt concentration of 0.02 mol$_c$ L^{-1} (reference case) and average root zone salinities that are approximately 3 times as large as C_z, the capillary upflowing water dilutes the root zone water, particularly if capillary upflow is relatively large, for shallow groundwater levels (Figure 7). This

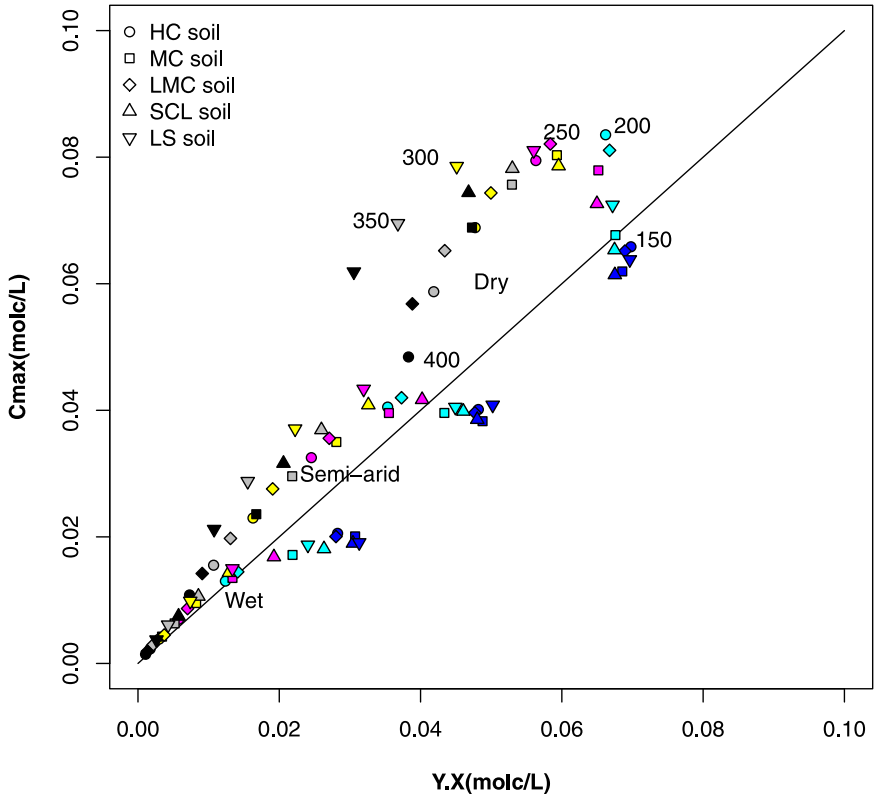

Figure 10. Comparison of C_{max} (the 84th percentile C value in the pdf) and YX (equation (11)) for six different groundwater depths and five different soil types (heavy clay soil, medium clay soil, light medium clay soil, sandy clay loam soil, and loamy sand soil; Table 1) under three different climates (dry climate, $\alpha\lambda/E_{max} = 0.89$; semiarid climate, $\alpha\lambda/E_{max} = 1.35$; and wet climate, $\alpha\lambda/E_{max} = 1.89$). The vegetation is trees (Table 2).

dilution is appreciable and is counteracted by removal of root zone water during dry spells. Incidental showers on a root zone with highly concentrated water after dry spells lead to a rapid loss of salts amounting to 25%–50% of the stock before the shower (Figure 4). Hence, the nonmonotone behavior of C as a function of Z is due to smaller concentrations in the root zone C by dilution with less saline groundwater if capillary upflow U is large (shallow groundwater) or due to small values of U (at deep groundwater) and leaching of saline root zone water. At groundwater depths where the dilution effect by upflowing groundwater becomes negligible, the largest concentrations are found as this volume becomes less significant (around $Z = 250$–300 cm) compared with root zone stored water but is still comparable to the leached water volumes.

[48] Looking at the long-term average concentrations in the root zone for different soil types, in Figure 6, a sequence is found for deeper groundwater levels that shows larger concentrations if the saturated hydraulic conductivity increases. The differences in the retention curves appear to be of secondary importance, as can be seen from the LMC and MC soils, which have virtually the same water retention curve but are shifted with regard to each other in Figure 6. Furthermore, the sequence is the same for deeper groundwater levels for all three climates. It is apparent that the soils with a larger saturated hydraulic conductivity (the main parameter in which these soils differ) show largest concentrations (the loss function of all soil types also confirms that net loss of water increases with the increase of hydraulic conductivity and subsequently causes larger concentrations), both for conditions where the root zone is more concentrated ($C/C_Z > 1$) and for conditions where concentrations are diluted compared with groundwater salinities (mainly wet climates). This suggests that the hydraulic conductivity is limiting with regard to upflow of brackish water, and the more limiting it is, the smaller root zone concentrations become.

[49] For shallow groundwater depths with wet conditions and for very large hydraulic conductivity (i.e., the LS soils), the hydraulic conductivity is not limiting. Here the salt accumulation becomes indifferent with respect to the soil type, or the reverse happens: larger hydraulic conductivities lead to smaller concentrations as less runoff and more infiltration occurs that dilutes root zone water and leaching is more efficient.

[50] As was mentioned before, the thickness of the root zone affects the leaching potential, as it is linearly related to the water volume as well as the salt mass that can be stored by the root zone. Because of this relationship, root zone thickness Z_r also influences surface runoff, which depends on the water storage volume that is still available to infiltrating water. We conducted simulations where we considered two alternatives: (1) runoff occurs as in all other calculations (default), or (2) runoff is added to

leaching. It appeared that runoff does not result in a significant effect. For thin root zones, where the water storage capacity is smallest and runoff should be most significant, changes were only up to 20% of the long-term averaged concentration in the root zone. For thicker root zones (50 or 100 cm), effects were negligible. Hence, runoff is discarded in the present analysis as a factor that might affect the salt accumulation. The insignificant effect of runoff on the root zone salt concentration can be explained by the low-frequency intensive showers that effectively decrease the root zone salt concentration. Adding runoff to the leaching flux (as a check on its impact) hardly increases salt leaching, as the root zone has already been rinsed.

[51] Also of importance is the impact of osmotic effects on the calculations. For the wet climate (Figure 7), it was ascertained that runoff explained about 50% of the relatively small C/C_Z difference between the root zone thickness of 25 cm and greater (50 or 100 cm). The remainder, which is only significant for groundwater salinities changing from 0.02 to 0.04, is due to osmotic effects. Hence, it is clear that osmotic effects start to play a role at a concentration of about 0.04 $mol_c\ L^{-1}$, as was mentioned earlier. For the dry climate, where salinity levels are larger, it is clear that besides the root zone thickness effect, the osmotic effects are also important (Figure 7): they shift the concentration levels up to larger values yet to smaller relative values (C/C_Z). This latter effect is due to osmotic effects on different water fluxes leading to larger root zone wetness and hence larger dilution (Figure 3).

[52] Although runoff does not appear to affect the results much, the reservoir size Z_r is important as fluctuations in fluxes become more attenuated when the reservoir increases. For the wet climate, it is plausible that "extreme events" are drought periods, and for the dry climate, extreme events would be wet, leaching periods. The impact of Z_r are consistent with that picture: in wet climates, thicker root zones attenuate drought effects and decrease the salinizing impact of large U and small L (evapotranspiration being quite constant). In dry climates, thicker root zones attenuate the capability of rain showers to rinse salts, leading to more saline conditions.

[53] We compared Figure 8 with the related analysis by *Suweis et al.* [2010]. Their Figure 2 showed the long-term average salt accumulation (in terms of salt concentrations) as a function of annual rainfall and rainfall frequency. As they ignored groundwater influences on the root zone water saturation and salinity, salt concentration levels depend only on the leaching potential of rainfall events. For their case, small showers may rewet the root zone but have little salt leaching potential, whereas large showers have a large leaching potential. In their analysis, salt enters the root zone through precipitation only. In our work, the rain is considered free of salt, and capillary flow from groundwater brings both water and salts to the root zone. Hence, if groundwater is sufficiently shallow to wet the root zone, most rain showers will cause leaching, and the leaching efficiency will improve if precipitation is distributed over more events. With larger and less frequent events, the system is less efficient at removing salts. Large events supply more water than is needed to flush the root zone, and the lower frequency of these events leads to a net increase in the salt concentrations. This implies that with increased climate variability (decrease in λ and increase in α) the influence of runoff becomes greater [*Entekhabi et al.*, 1992; *Kim*, 2005; *Milly*, 2001].

[54] Figure 9 shows that with a relatively simple approach, the dynamics (in terms of a mean concentration and a bandwidth around this average) can be reasonably approximated. Hence, if a rough indication is all that is needed, the demanding numerical computations may not be necessary. The limitation of this analytical approach is obvious: input was needed that can only be obtained by those demanding numerical computations, which one might want to avoid. This limitation may not be as prohibiting as it seems. If crops are concerned, the yield, which is easily measured, is well correlated with relative transpiration [*Rodriguez-Iturbe and Porporato*, 2004; *Shani et al.*, 2007]. This transpiration plus evaporation (controlled by irradiation, air humidity, leaf area index, and soil water saturation) should, over the long term, be derived from rainfall and capillary flux, where the first one can be measured relatively simply, evaporation can be reasonably well predicted, and the latter can therefore be calculated. Furthermore, the soil water status can be easily monitored.

[55] The pdfs of M and C react differently on Z and climate, and both are the result of opposing effects: wetness due to a wet climate or due to the proximity of groundwater favors leaching, the proximity of groundwater level also favors salt import by the root zone layer, and the water balance determines whether the capillary upflowing water U will concentrate or dilute the root zone with regard to salt concentration. For the long-term average fluxes, salt concentrations and mass converge to a mean value with irregular variations around this mean. However, salt inputs and outputs will balance; hence,

$$UC_z = LC \leftrightarrow \frac{C}{C_z} = \frac{U}{L},$$

and therefore, the values of these fluxes determine whether root zone concentrations will become larger or smaller than those in the groundwater. Many factors affect these fluxes, such as climate, groundwater depth, and soil type, and in view of opposing effects, salt accumulation in the root zone is a complex issue for sustainable planning of crop, soil, and groundwater, especially in semiarid regions [*Corwin et al.*, 2007]. In agreement with *Richards et al.* [1954], concentrations of 2, 4, and 8 mS cm^{-1} in terms of electrical conductivity (or 0.02, 0.04, and 0.08 $mol_c\ L^{-1}$ in terms of concentration or 1×10^5, 2×10^5, and 4×10^5 Pa in terms of osmotic pressure) are indicative of salt stress. These concentrations refer to salinity ranges in the saturated extract [see *Richards et al.*, 1954] for no adverse effects ($C < 0.02$), adverse effects for sensitive ($0.02 < C < 0.04$) and many plant species ($0.04 < C < 0.08$), and severe adverse effects where only tolerant plants show a good primary production ($C > 0.08$). The soil saturation in our analysis varies as a function of time, and moreover, the relationship between water content in the field and in the saturated extract depends on several soil properties in addition to soil saturation. For an impression, we indicate the gravimetric water content of the saturated paste extract (75% by weight of dry soil) and field capacity (25% by weight of dry soil [see also *Richards et al.,* 1954, Table 9.1]) as given by *Bolt*

and Bruggenwert [1976]. Apart from osmotic effects, root zone salinity cannot be considered to be a simple function of other factors, such as groundwater depth, root zone thickness, climate, and soil. However, if a rough indication suffices, a simple analysis may give a sufficiently accurate prediction.

[56] Though root zone fluxes vary as a function of time, on average, if capillary upflow is larger than leaching flux, it is probable that the salt concentration in the root zone becomes larger than the concentration in the groundwater. If capillary upflow is less than the leaching flux, salts entering the root zone may be flushed out effectively, and the concentration in the root zone remains below groundwater salt concentration. We conclude that if we know the groundwater depth, groundwater salinity, climate, and soil type, we can do a quick assessment of whether capillary upflow would be greater or less than the leaching flux and the resulting root zone salt concentration. Runoff may affect the overall water and salt balances. For a shallow root zone, the impact of runoff is larger than for a large root zone. For the presently considered cases, runoff was insignificant for the salt balance.

5. Conclusions

[57] Capillary groundwater fluxes influence the soil moisture balance in a limited range of groundwater levels, as was discussed by *Vervoort and van der Zee* [2008]. In their analysis, the impact of salt on the water balance was not considered. If groundwater is brackish or saline, the upward capillary fluxes carry along salt that may accumulate in the root zone. These salts may lead to a reduced transpiration because of the moisture stress caused by osmotic effects. In this paper, we consider the salt dynamics in the root zone and take osmotic effects on the water fluxes into account.

[58] The upward transport of salts from groundwater into the root zone is larger if the upward water flow rate is larger, but since it may also induce the root zone to become wetter on average and more prone to solute leaching events, the salt concentration that develops depends in a complex way on capillary upward flow. The long-term salt concentration is not a monotonically increasing or decreasing function of the various system parameters such as hydraulic conductivity, groundwater depth, or climate parameters. Dependencies can be different, as was shown by comparison of effects with those found by *Suweis et al.* [2010], where salt inputs were derived only from atmospheric deposition.

[59] Salt accumulation in the root zone is characterized by very erratic patterns of concentration and salt mass as a function of time, caused by the Poisson distributed daily rainfall. If we allow these patterns to stabilize, it is possible to determine the pdfs of important variables. If the stochasticity of weather is replaced by the average root zone water fluxes, a simple analytical approximation is feasible.

[60] **Acknowledgments.** Part of this research was done with funding by the Higher Education Commission of the government of Pakistan for S.H.H.S. and the Wageningen University IPOP program "Kust en Zee" and the Knowledge for Climate Research Program, Netherlands. We appreciate the funding by the Wageningen Institute of Environmental and Climate Research for the sabbatical visit of R.W.V. in Wageningen and the support of EPFL ENAC for the sabbatical visit of S.v.d.Z. to EPFL, Lausanne, Switzerland. A.R. and S.S. also acknowledge ERC Advanced grant RINEC-227612 and SFN grant 200021_124930/1.

References

Appelo, C. A. J., and D. Postma (2005), *Geochemistry, Groundwater and Pollution*, 2nd Edition, 649 pp., A. A. Balkema, Leiden, Netherlands.

Appels, W. M., P. W. Bogaart, and S. E. A. T. M. van der Zee (2011), Influence of spatial variations of microtopography and infiltration on surface runoff and field scale hydrological connectivity, *Adv. Water Resour.*, *34*, 303–313.

Berret-Lennard, E. G. (2003), The interaction between waterlogging and salinity in higher plants: Causes, consequences and implications, *Plant Soil*, *253*, 35–54.

Bolt, G. H. (1982), *Soil Chemistry*, 2nd ed., Elsevier, Amsterdam.

Bolt, G. H., and M. G. M. Bruggenwert (1976), *Soil Chemistry: A. Basic Elements*, 281 pp., Elsevier, Amsterdam.

Bras, R. L., and D. Seo (1987), Irrigation control in the presence of salinity: Extended linear quadratic approach, *Water Resour. Res.*, *23*(7), 1153–1161, doi:10.1029/WR023i007p01153.

Bresler, E. (1981), Transport of salts in soils and subsoils, *Agric. Water Manage.*, *4*, 35–62.

Bresler, E., B. L. MacNeal, and D. L. Carter (1982), Saline and sodic soils: Principles-Dynamics-Modeling, 236 pp., Springer-Verlag, New York.

Brooks, R. N., and A. T. Corey (1966), Properties of porous media affecting fluid flow, *J. Irrig. Drain. Div. Am. Soc. Civ. Eng.*, *92*(IR2), 61–68.

Caldwell, M. M., T. E. Dawson, and J. H. Richards (1998), Hydraulic lift: Consequences of water efflux from the roots of plants, *Oecologia*, *113*, 151–161.

Corwin, D. L., J. D. Rhoades, and J. Simunek (2007), Leaching requirements for soil salinity control: Steady-state versus transient models, *Agric. Water Manage.*, *90*, 165–180, doi:10.1016/j.agwat.2007.02.007.

Datta, K. K., and C. D. Jong (2002), Adverse effect of waterlogging and soil salinity on crop and land productivity in northwest region of Haryana India, *Agric. Water Manage.*, *57*, 223–238.

Dawson, T. E. (1993), Hydraulic lift and water use by plants: Implications for water balance, performance and plant-plant interactions, *Oecologia*, *95*, 565–574.

De Jong van Lier, Q., J. C. van Dam, K. Metselaar, R. de Jong, and W. H. M. Duijnisveld (2008), Macroscopic root water uptake distribution using a matric flux potential approach, *Vadose Zone J.*, *7*, 1065–1078, doi:10.2136/vzj2007.0083.

Domec, J. C., J. S. King, A. Noormets, E. Treasure, M. J. Gavazzi, G. Sun, and S. G. McNulty (2010), Hydraulic redistribution of soil water by roots affects whole-stand evapotranspiration and net ecosystem carbon exchange, *New Phytol.*, *187*, 171–183, doi:110.1111/j.1469-8137.2010.03245.x.

Eagleson, P. S. (Ed.) (2002), *Ecohydrology: Darwinian Expression of Vegetation Form and Function*, 496 pp., Cambridge Univ. Press, Cambridge, U. K.

Eagleson, P. S., (1978), Climate, soil, and vegetation: 3. A simplified model of soil moisture in the liquid phase, *Water Resour. Res.*, *14*(5), 722–730, doi:10.1029/WR014i005p00722.

Entekhabi, D., I. Rodriguez-Iturbe, and R. L. Bras (1992), Variability in large-scale water balance with land surface-atmosphere interaction, *J. Clim.*, *5*, 798–813.

Flowers, T. J., and T. D. Colmer (2008), Salinity tolerance in halophytes, *New Phytol.*, *179*, 945–963.

Green, S. R., B. E. Clothier, and D. J. McLeod (1997), The response of sap flow in apple roots to localised irrigation, *Agric. Water Manage.*, *33*, 63–78.

Guswa, A. J., M. A. Celia, and I. Rodriguez-Iturbe (2002), Models of soil moisture dynamics in ecohydrology: A comparative study, *Water Resour. Res.*, *38*(9), 1166, doi:10.1029/2001WR000826.

Guswa, A. J., M. A. Celia, and I. Rodriguez-Iturbe (2004), Effect of vertical resolution on predictions of transpiration in water-limited ecosystems, *Adv. Water Resour.*, *27*, 467–480, doi:10.1016/j.advwatres.2004.1003.1001.

Howell, T. A. (1988), *Irrigation Efficiencies: Handbook of Engineering in Agriculture*, pp. 173–184 pp., CRC Press, Boca Raton, Fla.

Isidoro, D., and S. R. Grattan (2011), Predicting soil salinity in response to different irrigation practices, soil types and rainfall scenarios, *Irrig. Sci.*, *29*, 197–211, doi:10.1007/s00271-00010-00223-00277.

Jalali, M., H. Merikhpour, M. J. Kaledhonkar, and S. E. A. T. M. van der Zee (2008), Effects of wastewater irrigation on soil sodicity and nutrient leaching in calcareous soils, *Agric. Water Manage.*, *95*, 143–153.

Kaledhonkar, M. J., N. K. Tyagi, and S. E. A. T. M. van der Zee (2001), Solute transport modelling in soil for irrigation field experiments with alkali water, *Agric. Water Manage.*, *51*, 153–171.

Katul, G. G., and M. B. Siqueira (2010), Biotic and abiotic factors act in coordination to amplify hydraulic redistribution and lift, *New Phytol.*, *187*, 3–6.

Kim, J. (2005), A projection of the effects of the climate change induced by increased CO_2 on extreme hydrologic events in the western U.S., *Clim. Change*, *68*, 153–168.

Kroes, J. G., J. C. van Dam, P. Groenendijk, R. F. A. Hendriks, and C. M. J. Jacobs (2008), SWAP version 3.2, theory description and user manual, 262 pp., Wageningen Univ. and Res. Cent., Wageningen, Netherlands.

Laio, F., A. Porporato, L. Ridolfi, and I. Rodriguez-Iturbe (2001), Plants in water-controlled ecosystems: Active role in hydrologic processes and response to water stress: II. Probabilistic soil moisture dynamics, *Adv. Water Resour.*, *24*, 707–723.

Laio, F., S. Tamea, L. Ridolfi, P. D'Odorico, and I. Rodriguez-Iturbe (2009), Ecohydrology of groundwater-dependent ecosystems: 1. Stochastic water table dynamics, *Water Resour. Res.*, *45*, W05419, doi:10.1029/2008WR007292.

Lamontagne, S., P. G. Cook, A. O'Grady, and D. Eamus (2005), Groundwater use by vegetation in a tropical savanna riparian zone (Daly River, Australia), *J. Hydrol.*, *310*, 280–293, doi:10.1016/j.jhydrol.2005.1001.1009.

Mensforth, L. J., P. J. Thorburn, S. D. Tyerman, and G. R. Walker (1994), Sources of water used by riparian *Eucalyptus camaldulensis* overlying highly saline groundwater, *Oecologia*, *100*, 21–28.

Milly, P. C. D. (2001), A minimalist probabilistic description of root zone soil water, *Water Resour. Res.*, *37*(3), 457–463, doi:10.1029/2000WR900337.

Minasny, B., and A. B. McBratney (2002), The efficiency of various approaches to obtaining estimates of soil hydraulic properties, *Geoderma*, *107*, 55–70.

Nadezhdina, N., et al. (2010), Trees never rest: The multiple facets of hydraulic redistribution, *Ecohydrology*, *3*, 431–444, doi:10.1002/eco.1148.

Oliveira, R. S., T. E. Dawson, S. S. O. Burgess, and D. C. Nepstad (2005), Hydraulic redistribution in three Amazonian trees, *Oecologia*, *145*, 354–363.

Pichu, R. (2006), World salinization with emphasis on Australia, *J. Exp. Bot.*, *57*(5), 1017–1023.

Porporato, A., F. Laio, L. Ridolfi, and I. Rodriguez-Iturbe (2001), Plants in water-controlled ecosystems: Active role in hydrologic processes and response to water stress: III. Vegetation water stress, *Adv. Water Resour.*, *24*, 725–744.

Raats, P. A. C. (1975), Distribution of salts in the root zone, *J. Hydrol.*, *27*, 237–248.

Rhoades, J. D. (1974), Drainage for salinity control, in *Drainage for Agriculture*, edited by J. Van Schilfgaarde, pp. 433–461, Soil Sci. Soc. of Am., Madison, Wis.

Rhoades, J. D., J. D. Oster, R. D. Ingvalson, J. M. Tucker, and M. Clark (1973), Minimizing the salt burdens of irrigation drainage waters, *J. Environ. Qual.*, *3*, 311–316.

Richards, L. A., L. E. Allison, L. Bernstein, C. A. Brown, J. W. Fireman, M. Hatcher, J. T. Hayward, H. E. Pearson, G. A. Reeve, and R. C. Wilcox (1954), *Diagnosis and Improvement of Saline and Alkali Soils, Agric. Handb.*, vol. 60, 160 pp., U.S. Dep. of Agric., Washington, D. C.

Ridolfi, L., P. D'Odorico, F. Laio, S. Tamea, and I. Rodriguez-Iturbe (2008), Coupled stochastic dynamics of water table and soil moisture in bare soil condition, *Water Resour. Res.*, *44*, W01435, doi:10.1029/2007WR006707.

Rodriguez-Iturbe, I., and A. Porporato (2004), *Ecohydrology of Water-Controlled Ecosystems: Soil Moisture and Plant Dynamics*, Cambridge Univ. Press, Cambridge, U. K.

Rodriguez-Iturbe, I., V. K. Gupta, and E. Waymire (1984), Scale considerations in the modeling of temporal rainfall, *Water Resour. Res.*, *20*(11), 1611–1619, doi:10.1029/WR020i011p01611.

Rodriguez-Iturbe, I., A. Porporato, L. Ridolfi, V. Isham, and D. R. Cox (1999), Probabilistic modelling of water balance at a point: The role of climate soil and vegetation, *Proc. R. Soc. London, Ser. A*, *455*, 3789–3805.

Rozema, J., and T. Flowers (2008), Crops for a salinized world, *Science*, *322*, 1578–1582.

Runyan, C. W., and P. D'Odorico (2010), Ecohydrological feedbacks between salt accumulation and vegetation dynamics: Role of vegetation-groundwater interactions, *Water Resour. Res.*, *46*, W11561, doi:10.1029/2010WR009464.

Schoups, G., and J. W. Hopmans (2002), Analytical model for vadose zone solute transport with root water and solute uptake, *Vadose Zone J.*, *1*, 158–171.

Scott, R., T. E. Huxman, D. G. Williams, and D. C. Goodrich (2006), Ecohydrological impacts of woody-plant encroachment: Seasonal patterns of water and carbon dioxide exchange within a semiarid riparian environment, *Global Change Biol.*, *12*, 311–324, doi:10.1111/j.1365-2486.2005.01093.x.

Shani, U., A. Ben-Gal, E. Tripler, and L. M. Dudley (2007), Plant response to the soil environment: An analytical model integrating yield, water, soil type, and salinity, *Water Resour. Res.*, *43*, W08418, doi:10.1029/2006WR005313.

Simunek, J., D. L. Suarez, and M. Sejna (1996), The UNSATCHEM software package for simulating one-dimensional variably saturated water flow, heat transport, carbon dioxide production and transport, and solute transport with major ion equilibrium and kinetic chemistry, version 2, *Res. Rep. 141*, 186 pp., U.S. Salinity Lab., Riverside, Calif.

Simunek, J., M. Sejna, and M. T. van Genuchten (1998), The HYDRUS-ID software package for simulating the one-dimensional movement of water, heat and multiple solutes in variably saturated media, Version 2.0, *Rep. IGWMC-TPS-70*, Int. Ground Water Model. Cent., Colo. Sch. of Mines, Golden.

Simunek, J., M. Sejna, and M. T. van Genuchten (1999), The HYDRUS-2D software package for simulating the two-dimensional movement of water, heat, and multiple solutes in variably saturated media, Version 2.0, *Rep.* IGWMC-TPS-53, *Int. Ground Water Model. Cent.*, Colo. Sch. of Mines, Golden, Colo.

Somma, F., J. W. Hopmans, and V. Clausnitzer (1998), Transient three-dimensional modeling of soil water and solute transport with simultaneous root growth, root water and nutrient uptake, *Plant Soil*, *202*, 281–293.

Suweis, S., A. Rinaldo, S. E. A. T. M. van der Zee, A. Maritan, and A. Porporato (2010), Stochastic modeling of soil salinity, *Geophys. Res. Lett.*, *37*, L07404, doi:10.1029/2010GL042495.

Szabolcs, I. (1989), *Salt Affected Soils*, 274 pp., CRC Press, Boca Raton, Fla.

Tamea, S., F. Laio, L. Ridolfi, P. D'Odorico, and I. Rodriguez-Iturbe (2009), Ecohydrology of groundwater-dependent ecosystems: 2. Stochastic soil moisture dynamics, *Water Resour. Res.*, *45*, W05420, doi:10.1029/2008WR007293.

Teuling, A. J., and P. A. Troch (2005), Improved understanding of soil moisture variability dynamics, *Geophys. Res. Lett.*, *32*, L05404, doi:10.1029/2004GL021935.

Thorburn, P. J., and G. R. Walker (1994), Variations in stream water uptake by *Eucalyptus camaldulensis* with differing access to stream water, *Oecologia*, *100*, 293–301.

Toth, T. (2008), Salt-affected soils in Hungary, in *Needs and Priorities for Research and Education in Biotechnology Applied to Emerging Environmental Challenges in SEE Countries: Workshop Proceedings,* edited by G. Crescimanno et al., pp 75–81, UNESCO-BRESCE, Venice, Italy.

Toth, T., and G. Szendrei (2006), Types and distribution of salt affected soils in Hungary, and the characterisation of the processes of salt accumulation (in Hungarian), *Topogr. Mineral. Hungariae*, *IX*, 7–20.

Van Beek, C. L., et al. (2010), The need for harmonizing methodologies for assessing soil threats in Europe, *Soil Use Manage.*, *26*, 299–309.

van der Zee, S. E. A. T. M., S. H. H. Shah, C. G. R. Van Uffelen, P. A. C. Raats, and N. dal Ferro (2010), Soil sodicity as a result of periodical drought, *Agric. Water Manage.*, *97*, 41–49, doi:10.1016/j.agwat.2009.08.009.

Varrallyay, G. (1989), Soil mapping in Hungary, *Agrokemiaes Talajtan*, *38*, 696–714.

Vervoort, R. W., and S. E. A. T. M. van der Zee (2008), Simulating the effect of capillary flux on the soil water balance in a stochastic ecohydrological framework, *Water Resour. Res.*, *44*, W08425, doi:10.1029/2008WR006889.

Vervoort, R. W., and S. E. A. T. M. van der Zee (2009), Stochastic soil water dynamics of phreatophyte vegetation with dimorphic root systems, *Water Resour. Res.*, *45*, W10439, doi:10.1029/2008WR007245.

Walker, J., F. Bullen, and B. G. Williams (1993), Ecohydrological changes in the Murray-Darling Basin. I—The number of trees cleared over two centuries, *J. Appl. Ecol.*, *30*, 265–273.

Whitehead, D., and C. L. Beadle (2004), Physiological regulation of productivity and water use in *Eucalyptus*: A review, *For. Ecol. Manage.*, *193*, 113–140.

A. J. Guswa, Picker Engineering Program, Smith College, 100 Green St., Northampton, MA 01060, USA.

A. Rinaldo and S. Suweis, Laboratory of Ecohydrology, IEE, ENAC, École Polytechnique Fédérale, CH-1015 Lausanne, Switzerland.

S. H. H. Shah and S. E. A. T. M. van der Zee, Soil Physics, Ecohydrology and Groundwater Management, Environmental Sciences Group, Wageningen University, PO Box 47, NL-6700 AA Wageningen, Netherlands. (syed.shah@wur.nl)

R. W. Vervoort, Hydrology Research Laboratory, Faculty of Agriculture, Food and Natural Resources, University of Sydney, Sydney, NSW 2006, Australia. (willem.vervoort@sydney.edu.au)